



HAL
open science

On the feasibility of defect detection in composite material based on thermal periodic excitation

B. Lascoup, Laetitia Perez, Laurent Autrique, Antoine Crinière

► To cite this version:

B. Lascoup, Laetitia Perez, Laurent Autrique, Antoine Crinière. On the feasibility of defect detection in composite material based on thermal periodic excitation. *Composites Part B: Engineering*, 2013, 45, pp.1023-1030. hal-00845958

HAL Id: hal-00845958

<https://hal.science/hal-00845958>

Submitted on 18 Jul 2013

HAL is a multi-disciplinary open access archive for the deposit and dissemination of scientific research documents, whether they are published or not. The documents may come from teaching and research institutions in France or abroad, or from public or private research centers.

L'archive ouverte pluridisciplinaire **HAL**, est destinée au dépôt et à la diffusion de documents scientifiques de niveau recherche, publiés ou non, émanant des établissements d'enseignement et de recherche français ou étrangers, des laboratoires publics ou privés.

**On the feasibility of defect detection in composite material based on
thermal periodic excitation**

Bertrand Lascoup¹, Laetitia Perez², Laurent Autrique^{3*} and Antoine Crinière⁴

¹ ESTACA Campus ouest, Laboratoire Structure et Matériaux, rue Georges Charpak,
53000 Laval, France, bertrand.lascoup@estaca.fr

² Laboratoire de Thermocinétique de Nantes – UMR CNRS 6607, rue Christian Pauc,
44306 Nantes Cedex 03, France, laetitia.perez@univ-nantes.fr

³ Laboratoire d'Ingénierie des Systèmes Automatisés, ISTIA, 62 avenue notre dame du
lac, 49000 Angers, France, laurent.autrique@univ-angers.fr

⁴ IFSTTAR, MACS, route de Bouaye, CS4, 44344 Bouguenais Cedex, France,
antoine.crinieri@ifsttar.fr

* Author to whom correspondence should be addressed, Tel: +33 241 226 518,
Fax: +33 241 226 561

ABSTRACT: Implementation of periodic thermal excitation to identify thermal properties (conductivity, heat capacity, diffusivity) of complex composite materials at different investigation scales (from micrometer to millimetre) presents many advantages. These methods are usually based on the thermal waves phase lag observation compared to a reference signal. In fact, phase lag evolution versus distance to the heating source or versus excitation frequency is quite informative about numerous material characteristics. For example, considering that a structural defect can modify heat propagation inside a material, diagnosis can be performed from phase lag observations and comparisons between samples with and without defects. Numerous studies have been performed considering global heating (a quite large surface of the investigated composite material is heated and defect depth or size can be detected). The proposed approach is original since periodic heating is local and aims to detect defects in the periphery of the excitation. Based on a mathematical model for thermal waves propagations and introducing complex temperature for numerical resolution (finite element method), a feasibility study has allowed a sensitivity analysis. This preliminary study also provides information on the operating protocol, for heating (frequency, power, size of the source), and observation (transmission or reflection). Then, experimental device and early experimental results are briefly exposed.

Keywords: Non destructive testing (D), Defects (B), Modulated photothermal method.

1. INTRODUCTION

Nowadays increasing use of polymer composite materials reinforced by fibres (carbon or glass) is required in many industrial processes because of their combination of high stiffness and high strength with low density. Moreover, low production cost can be obtained through the ability to manufacture unique complex components in single operations with minimal material wastage and reducing the number of junction between parts while a classical metallic structure may need bolting, riveting or welding. Main end-users of this type of complex composite materials are transport industries such as automotive, aeronautical as well as railway domain. Others benefits of the use of composite materials include their better mechanical strength, their efficient corrosion resistance and their quality from the fatigue behaviour point of view. However, for any structure dedicated to a specific application, an accurate control of its properties and structure health monitoring (assembly, bound, resin & fibre) are required to guarantee their quality. Actually numerous defect determinations inside a composite material are carried out using acoustic techniques requiring a fluid vector which can deteriorate or pollute the material [1]. To limit the potential contamination of the sample, several non destructive processes based on the observation of the thermal behaviour induced by a heating step have already been investigated. The observations of the thermal scene using an infra-red camera allow to reveal defects (even deep one). In this context, several studies can be mentioned: [2] for crack detection at micrometric scale, [3] for recent applications of detection of defects in civil engineering and finally [4] for a comparison with various techniques of defects detection in metallic structures. However, such an approach requires non-negligible thermal energy which can induce material deterioration. An attractive idea is to develop a method based on the analysis of

the propagation of low energetic thermal waves in a sample using a periodic excitation. Indeed, relevant information could be collected from a modulated heating of reduced energy (compared to a classical flash method for example). In the literature, various implementations of this approach (called modulated photothermy) can be found for parametric identification. Indeed in [5] this method is used to identify thermal conductivity tensor of orthotropic materials; in [6] identification of thermal diffusivity of fibre embedded in matrix is investigated, and in [7] numerous experimental devices related to the periodic method are presented (allowing investigations from micrometer scale to decimetre scale). Although the key parameter conditioning the thermal wave propagation is the material thermal diffusivity, the use of periodic method to detect defect appears particularly attractive by avoiding the considered material deterioration. Recently, these techniques were implemented for defects detection [8] or damage characterization in an aircraft composite [9]. In [10], an application of modulated thermography is discussed to find defects in a mural paint (XIVth century) before its restoration. In [11], a recent application in civil engineering is also exposed. In this paper, the principle of periodic method is exposed and the mathematical model satisfied by temperature expressed in its complex formalism is presented. Based on numerical simulations, the sensitivity of the model to nuisance parameters and the feasibility of heterogeneities detection for an isotropic and/or orthotropic material are detailed. Finally, the specific experimental device is presented and first experimental results are described. A conclusion summarizes the main results and lists potential prospects.

2. MODELING OF THE MODULATED PHOTOTHERMAL EFFECT

In this paragraph the equations governing the propagation of thermal waves within a material are presented. The notion of complex temperature is also introduced. Finally results of numerical simulations are presented and the effects of nuisance parameters are discussed.

2.1 Equations

In this section only the case of the surface absorption of modulated laser light is investigated. Let us consider a 3-D plane material (Figure 1). The plate is denoted by Ω (e is the sample thickness) ; X is the space variable, $X = (x, y, z) \in \Omega \subset \mathbb{R}^3$ and $t \in T$ is the time. $\partial\Omega$ is the boundary of Ω . Initial temperature θ_{amb} is assumed to be homogeneous and equal to the surrounding environment temperature. The increase of the temperature from the initial state at any time $t \in T$ and at any point $X \in \Omega$ when one of the boundary $\Gamma \subset \partial\Omega$ is excited by a periodical signal $\Phi(X, t)$ is defined by $\theta_0(X, t)$ and is governed by the following system of partial differential equations (PDE):

$$\forall (X, t) \in \Omega \times T \quad C \frac{\partial \theta_0(X, t)}{\partial t} - \lambda \Delta \theta_0(X, t) = 0 \quad (1)$$

$$\forall (X, t) \in \Gamma \times T \quad -\lambda \frac{\partial \theta_0(X, t)}{\partial \vec{n}} = h \theta_0(X, t) - \Phi(X, t) \quad (2)$$

$$\forall (X, t) \in (\partial\Omega / \Gamma) \times T \quad -\lambda \frac{\partial \theta_0(X, t)}{\partial \vec{n}} = h \theta_0(X, t) \quad (3)$$

$$\forall X \in \Omega \quad \theta_0(X, 0) = 0 \quad (4)$$

where C is the volumetric heat $[\text{J.m}^{-3}.\text{K}^{-1}]$, λ the thermal conductivity $[\text{W.m}^{-1}.\text{K}^{-1}]$, \vec{n} is the unit normal vector of $\partial\Omega$ and h is the convective heat transfer coefficient $[\text{W.m}^{-2}.\text{K}^{-1}]$. When a solid medium is subjected to a periodic excitation, its temperature aims towards a periodic regime after a transient state. Thus, in steady state the thermal wave at each point is characterized by the amplitude of the oscillations noted $M(X)$ and a phase lag from a reference signal noted $\varphi(X)$ (Figure 1).

Introducing the notion of complex temperature (illustrated for example in [5-7]), a new system of PDE is considered:

$$\forall X \in \Omega \quad j\omega C \tilde{\theta}(X) - \lambda \Delta \tilde{\theta}(X) = 0 \quad (5)$$

$$\forall X \in \Gamma \quad -\lambda \frac{\partial \tilde{\theta}(X)}{\partial \vec{n}} = h \tilde{\theta}(X) - \tilde{\Phi}(X, t) \quad (6)$$

$$\forall X \in (\partial\Omega / \Gamma) \quad -\lambda \frac{\partial \tilde{\theta}(X)}{\partial \vec{n}} = h \tilde{\theta}(X) \quad (7)$$

The complex solution $\tilde{\theta}(X)$ of the system (Equations (5) to (7)) gives at each point the modulus $M(X) = |\tilde{\theta}(X)|$ and the phase lag $\varphi(X) = \arg(\tilde{\theta}(X))$ of the fundamental harmonic (compared with the fundamental harmonic of the input reference signal $\Phi(X, t)$). It is important to note that system (Equations (5) to (7)) no longer depends on time which significantly reduces computation time of the numerical resolution using a finite element method (FEM). Moreover, in one-dimensional case the problem in such statement was formulated and solved analytically in [12-14].

It is well known [5-7] that from both observable data (amplitude and phase lag) the amplitude is the most subjected to noise and to external disturbances. Furthermore amplitude mostly depends on the power of the heating flux while the phase lag does not depend on it. In order to obtain reliable data, the diffusion length μ in [m] has to be defined in order to inform about the effect of the thermal wave in the sample: $\mu = \sqrt{\alpha/(\pi f)}$ with $\alpha = \lambda/C$ the thermal diffusivity in [m².s⁻¹] and f the frequency in [Hz]. It is usual to consider that at a distance up to 3μ the thermal wave amplitude falls down. The consequence is the relation between sample thickness and possible excitation frequencies for a given material. When the thickness increases, the signal to noise ratio decreases on the opposite. To illustrate the model presented in this section, several numerical simulation results are presented below.

2.2 Data analysis

Different methods can be implemented and various options are proposed:

- Transmission or reflection: in transmission, temperature measurement and excitation are performed on opposite face of the sample. In specific situations, if the opposite face is not accessible to measurements, observations are performed on the same sample side (reflection).
- Spatial scanning or frequency scanning. Considering a spatial scanning, the phase lag of the thermal wave is observed along the distance of the excitation centre for a given frequency. If the thermal behaviour is observed at a fixed point while a frequency range is scanning, a frequency scanning is considered.

Thus, four modes of analysis can be retained. For experimental reasons (see last section) spatial scanning in transmission will be considered thereafter.

2.3 Numerical simulations

Numerical simulation results presented below correspond to two configurations. For the first one a conductive isotropic material is investigated while for the second one an orthotropic material (carbon fibres embedded in epoxy resin) is considered. Heating source spatial distribution on the excited face is assumed to be a disk of 5 mm radius and a power of $10^5 \text{ [W.m}^{-2}\text{]}$. The exchange coefficient due to natural convection is assumed to be equal to $h = 15 \text{ [W.m}^{-2}\text{.K}^{-1}\text{]}$. Experimental data are presented in Table 1. In the following figures, phase lag and amplitude distributions of the thermal waves on the unheated face in transmission are plotted considering both materials. When the signal is too weak $M(X) = |\tilde{\theta}(X)| < 0.1^\circ\text{C}$ to be informative, the phase lag $\varphi(X) = \arg(\tilde{\theta}(X))$ is not determined. Numerical results are obtained using Comsol® software.

In Figure 2, considering an isotropic material sample (titanium) and a 0.1 Hz excitation frequency (10s period), an amplitude of 40K is obtained in the sample centre. Furthermore, orthotropy of the considered composite material is highlighted by elliptic curves of both phase lag and modulus. Such shapes are specific of orthotropic material and are due to fibres orthogonal directions. These simulation results could be also used preliminary to any experimental campaign to ensure that the signal is exploitable. If the diffusion length is not large enough the frequency must be reduced.

2.4 Effect of nuisance parameters

In order to optimize the identification methodology and the experimental bench, sensitivity analysis is a crucial requirement. Sensitivity analysis quantifies the effect of each input parameter of the model $p \in \{\alpha, h, \Phi, e, f\}$ on the output parameters (modulus and phase lag). In the case of isotropic material (titanium) whom data are presented in Table 1 the reduced sensitivities $p \frac{\partial M(X)}{\partial p}$ and $p \frac{\partial \varphi(X)}{\partial p}$ versus distance are plotted in the following figure (Figure 3). In the considered configuration, inaccuracies on convective exchange (h) estimation do not affect modulus and phase lag of thermal wave while the material thickness and the excitation frequency have to be known with great accuracy. Moreover, heating source amplitude has a real influence on the temperature oscillations modulus while it has no influence on the phase lag. Finally, thermal diffusivity is a key parameter considering the thermal wave propagation. The same considerations can be made for orthotropic materials [5].

In the following section, the previous predictive numerical tool dedicated to the resolution of the PDE system (Equations 5–7) is implemented in order to detect defect inside the investigated sample.

3. NUMERICAL STUDY OF FEASIBILITY

In this section, the effect of a defect on the distribution of the thermal wave is highlighted. The difference of the thermal behaviour considering modulus and phase lag between a "healthy" material and a "defective" material is shown using numeric simulations. A spatial scanning in transmission is considered. The power of the 5 mm radius spatial distribution of the heating source is equal $10^4 \text{ [W.m}^{-2}\text{]}$. This thermal

excitation is located at the centre of the sample upper face $(0, 0, 0)$ and the convective exchange coefficient is assumed to be equal to $h = 15 \text{ [W.m}^{-2}\text{.K}^{-1}\text{]}$.

3.1 Inclusion detection

The healthy material is a 3 mm thick polymer. It contains a glass disk 1mm thick and 5mm radius as inclusion. The inclusion centre is located at the point $(1.5, 10, 0)$ (in mm). Excitation frequency is fixed at 0.001 Hz. Thermal properties of healthy material and inclusion are detailed in the Table 2.

Differences between thermal behaviour of healthy and defective materials are plotted in Figure 4. The presence of a defect can be observed on both modulus and phase lag spatial distributions. However, it is quite difficult to estimate by visual assessment shape, depth, thickness or nature of the defect.

3.2 Detection of a fibres misalignment

The healthy material is the composite material considered previously (section 2.3) made of carbon fibres embedded in a 3 mm thick epoxy resin. The 1 mm thick defect corresponds to a 1 cm^2 square patch which the fibres orientation is orthogonal to the fibres orientation of the whole material. The defect centre is located at the point $(1.5, 10, 0)$ (in mm). The excitation frequency is fixed at 0.005 Hz. Thermal properties of healthy material and patch are detailed in Table 3.

Differences between thermal behaviour of healthy and defective composite materials are plotted in Figure 5. The presence of the defect (90° angle misalignment of carbon fibre)

significantly modifies the thermal wave distribution. Thus detection by analyzing differences of modulus and phase lag is meaningful.

4. FIRST EXPERIMENTAL CAMPAIGN

The previous numerical results have shown that the analysis of the thermal waves propagation generated by a periodical solicitation could lead to the detection of defects within composite materials. An experimental device developed based on this principle and the first experimental results performed on composite materials with a defined kind of heterogeneity are presented in this section.

4.1 Experimental device (modulated phototherapy)

An experimental specific device has been developed in order to validate the previous method which allows to detect defects. This experimental bench comprises three main parts (Figure 6): an infra-red camera Flir A20, a halogen lamp (radiative heating source) and a Köhler optical device to insure a uniform spatial distribution of the heating source. The sample is located in the focal plane of this Köhler optical device. Pioneer works was published in 1893 by Köhler [15-16].

From the experimental point of view, several steps can be considered:

- Tests on a reference sample without defects are preliminary performed. Temperature observations using infra red camera inform about isotropic, anisotropic or othotropic properties of the sample. Halogen lamp power supply is chosen in order to avoid high temperature on the heated face (maximum temperature threshold depends on investigated material physical properties).

- Excitation frequency is adjusted in order to obtain a relevant signal to noise ratio on the non heated face (spatial scanning in transmission). This frequency depends on the material diffusivity (diffusion length), the plate thickness and the heating source radius. From their own experiences, authors usually start experimental investigations with a heating source radius equal to the plate thickness and choose an excitation frequency such that the diffusion length is equal to the sample thickness. For such a start point, material thermal diffusivity has to be a priori known (otherwise identification process can be previously implemented [5]).
- In order to estimate both modulus and phase lag spatial distribution a lock-in algorithm is implemented. Recording duration has to be greater than 10 periods (with at least 50 images per period).

4.2 First experimental results

A 30x40cm² carbon-epoxy orthotropic sample (Figure 6), 1.7 mm thick has been performed at the Laboratory of Structure and Materials (ESTACA - Laval - France). This sample is composed of seven plies and defects have been integrated in the middle of the stacking. The following results correspond to the detection of a 1 cm² square, 0.2 thick copper defect within a carbon epoxy orthotropic material. For this experimental transmission configuration, the excitation frequency is 0.048 Hz and the heating source spatial distribution radius is about 3.6 mm. The halogen lamp power is 300 W. Figure 7 shows modulus and phase lags cartographies for a healthy zone and defect zone of the considered sample. Moreover, both modulus and phase lags differences are plotted. The

presence and the position of the defect are unmistakably detected considering that the measurement confidence is about 0.2°C for modulus and about 5° for phase lag.

5. CONCLUSION

In this paper, a non-destructive approach for defect detection in composite materials has been proposed. Based on the analysis of system state behaviour when submitted to a modulated input, a periodic methodology has been presented: forward model, sensitivity analysis, numerical validation, experimental device and experimental validation. The main advantage of this technique is to be used even if the signal versus noise (on observable output) ratio is low and thus to preserve the material integrity. This last point is particularly interesting in numerous applications in biomedical engineering where tested tissues cannot undergo an important temperature rise.

Several outlooks can be considered. Different typical defects have to be tested. In particular, modifications of structures (due to a mechanical impact for example) could be studied. Beyond the detection of a possible defect and the estimation of its position, it must be useful to characterise its nature and its geometry. An inverse method based on the analysis of the differences of the modulus and the phase lags has to be implemented by minimizing a quadratic criterion by an iterative procedure (Levenberg-Marquardt algorithm for example).

6. REFERENCES

- [1] Hasiotis, T., Badogiannis, E. and Tsouvalis, N.G. Application of Ultrasonic C-Scan Techniques for Tracing Defects in Laminated Composite Materials Cracks

detection by a moving photothermal probe, 4th international conference on Non Destructive Testing, Crete, Greece, 11-14 October 2007.

- [2] Bodnar, J.L., Egee, M., Menu, C., Besnard, R., Le Blanc, A., Pigeon, M. and Sellier, J.Y. Cracks detection by a moving photothermal probe, *Journal de physique IV*, C7, 4, July 1994.
- [3] Marchetti, M., Ludwig, S., Dumoulin, J., Ibos, L. and Mazioud, A. Active infrared thermography for non-destructive control for detection of defects in asphalt pavements, 9th international conference on quantitative infrared thermography, Krakow, Poland, 2-5 July 2008.
- [4] Maillard, S., Cadith, J., Eschimese, D., Walaszek, H., Mooshofer, H., Candore, J.C. and Bodnar, J.L. Towards the use of passive and active infrared thermography to inspect metallic components in the mechanical industry, 10th international conference on quantitative infrared thermography, Québec, Canada, 27-30 July 2010.
- [5] Perez, L. and Autrique, L. Robust determination of thermal diffusivity values from periodic heating data, *Inverse Problems IOP journal*, 25(4), pp. 45011-45031, 2009.
- [6] Autrique, L., Perez, L. and Serra, J.J. Finite element modelling for microscale thermal investigations using photothermal microscopy data inversion, *Measurement Science Technology*, 18, pp. 1-11, 2007.
- [7] Autrique, L., Perez, L. and Scheer, E. On the use of periodic photothermal methods for material diagnosis, *Sensors and Actuators B*, 135(2), pp. 478-487, 2009.

- [8] Ishikawa, M., Hattal, H., Habuka, Y., Jinnai, S., Utsunomiya, S. and Goto, K. Pulse-phase-thermographic non-destructive testing for CRFP specimen; 14th European conference on composite materials, Budapest, Hungary, 7-10 June 2010.
- [9] Grammatikos, S.A., Kordatos, E.Z., Barkoula, N.M., Matikas, T. and Paipetis, A. Innovative non-destructive evaluation and damage characterization of composite aerostructures, 14th European conference on composite materials, Budapest, Hungary, 7-10 June 2010.
- [10] Candore, J.C., Szatanik, G., Bodnar, J.L., Detalle, V. and Grossel, P. Infra-red photothermal thermography : A tool of assistance for the restoration of murals paintings ?, 8th international conference on quantitative infrared thermography, 37 (in cd), Padova, Italie, 28-30 June 2006.
- [11] Sakagami, T., Izumi, Y., Mori, N. and Kubo, S. Development of self-reference lock-in thermography and its application to remote nondestructive inspection of fatigue cracks in steel bridges, 10th international conference on quantitative infrared thermography, Québec, Canada, 27-30 July 2010.
- [12] Gonzalez de la Cruz, G. and Gurevich, Y.G. Thermal Diffusion of a Two Layer System, *Physical Review B*, 1995, 51, pp. 2188-2192, 1995.
- [13] Gonzalez de la Cruz, G. and Gurevich, Y.G. Physical Interpretation of Thermal Waves in Photothermal Experiments, *Revista Mexicana de Fisica*, 45(1), pp. 41-46, 1999.
- [14] Gurevich, Y.G., Logvinov, G. and Lashkevich, I. Boundary Conditions in Theory of Photothermal Processes in Solid, *Review of Scientific Instruments*, 74(1), pp. 589—591, 2003.

- [15] Köhler, A. Ein neues Beleuchtungsverfahren für mikrographische Zwecke, Zeitschrift für wissenschaftliche Mikroskopie und für Mikroskopische Technik, 10(4), pp. 433–440, 1893.
- [16] Köhler, A. New Method of Illumination for Photomicrographical Purposes, Journal of the Royal Microscopical Society; 14, pp. 261–262, 1894.

	Isotropic material (titanium)	Orthotropic material
Thermal conductivity λ [W.m ⁻¹ .K ⁻¹]	21.6	$\begin{bmatrix} 1 & 0 & 0 \\ 0 & 5 & 0 \\ 0 & 0 & 1 \end{bmatrix}$
Volumetric heat capacity C [J.m ⁻³ .K ⁻¹]	2.4 · 10 ⁶	1.6 · 10 ⁶
Frequency [Hz]	0.1	0.05
Diffusion length μ	≈ 5 mm	2 ≤ μ ≤ 5 mm
Thickness e	1 mm	3 mm

Table 1 Input parameters used in simulations

	Thermal conductivity [W.m ⁻¹ .K ⁻¹]	Volumetric heat capacity [J.m ⁻³ .K ⁻¹]
Polymer sample	0.24	1.7 · 10 ⁶
Glass defect	1.38	1.5 · 10 ⁶

Table 2 Data used in the mathematical model for inclusion detection

	Thermal conductivity	Volumetric heat capacity
	$[\text{W.m}^{-1}.\text{K}^{-1}]$	$[\text{J.m}^{-3}.\text{K}^{-1}]$
Global composite	$\begin{bmatrix} 1 & 0 & 0 \\ 0 & 5 & 0 \\ 0 & 0 & 1 \end{bmatrix}$	$1.6 \cdot 10^6$
Fibres misalignment	$\begin{bmatrix} 1 & 0 & 0 \\ 0 & 1 & 0 \\ 0 & 0 & 5 \end{bmatrix}$	$1.6 \cdot 10^6$

Table 3 Technical data used in the model representing a misalignment of fibres

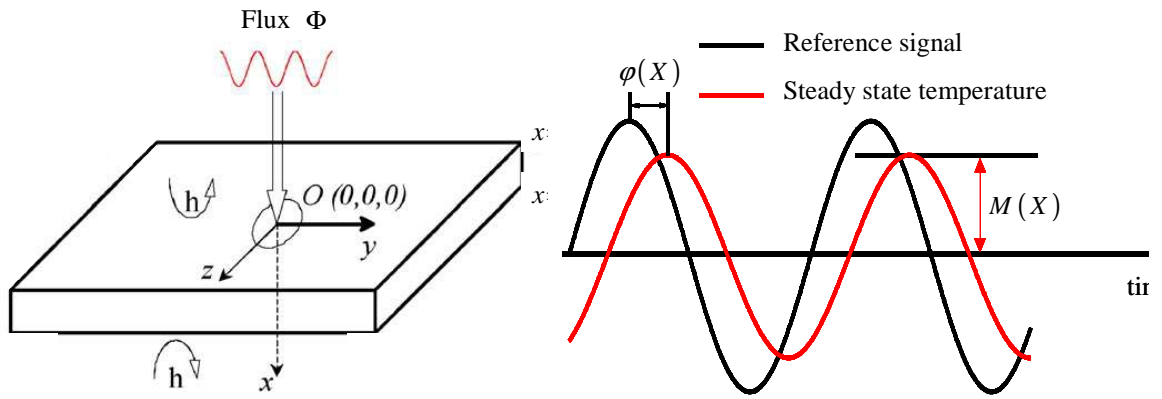


Figure 1 Considered geometry and representation of temperature evolutions in steady state

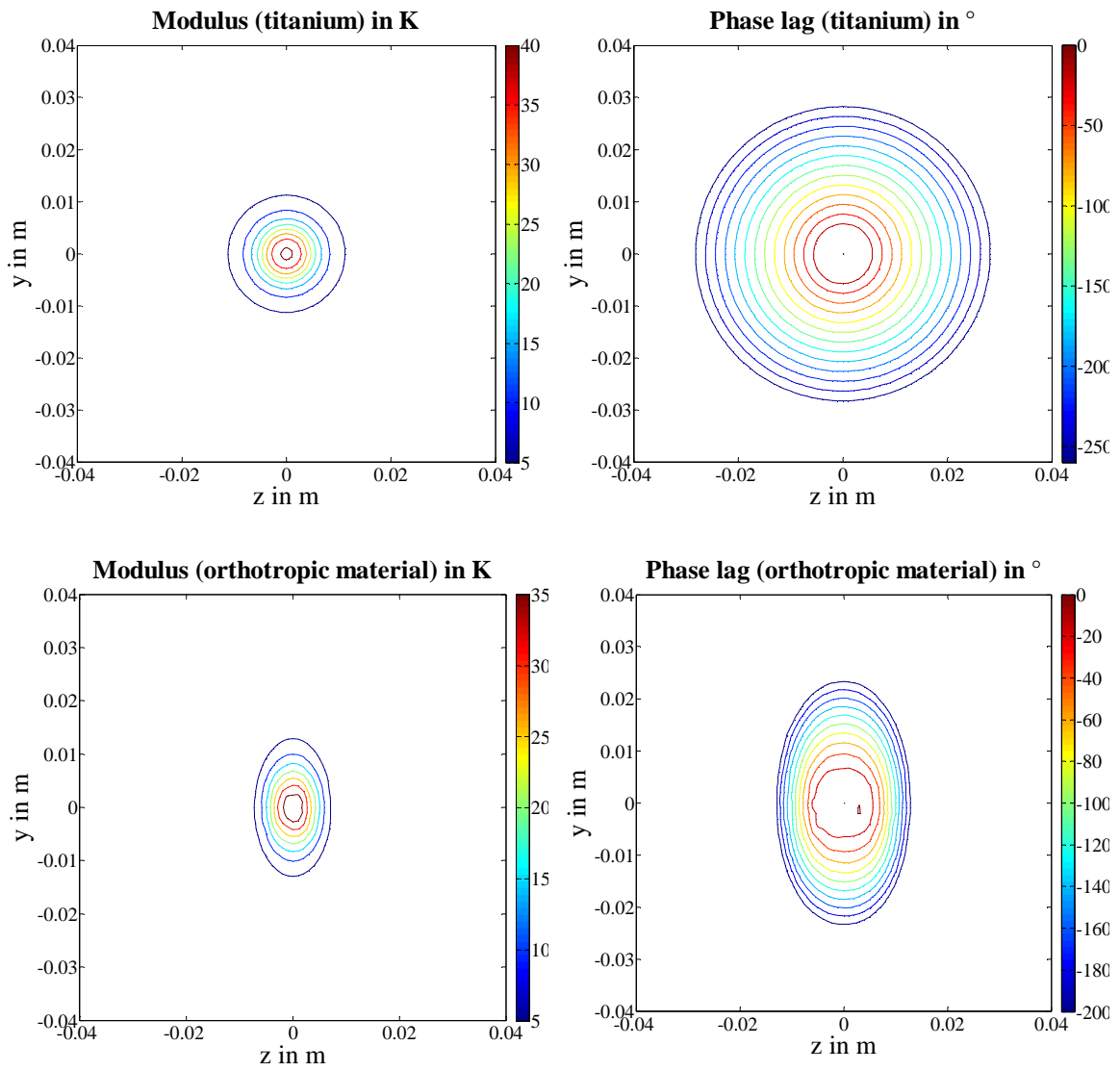


Figure 2 Simulated modulus and phase lag for titanium and orthotropic material

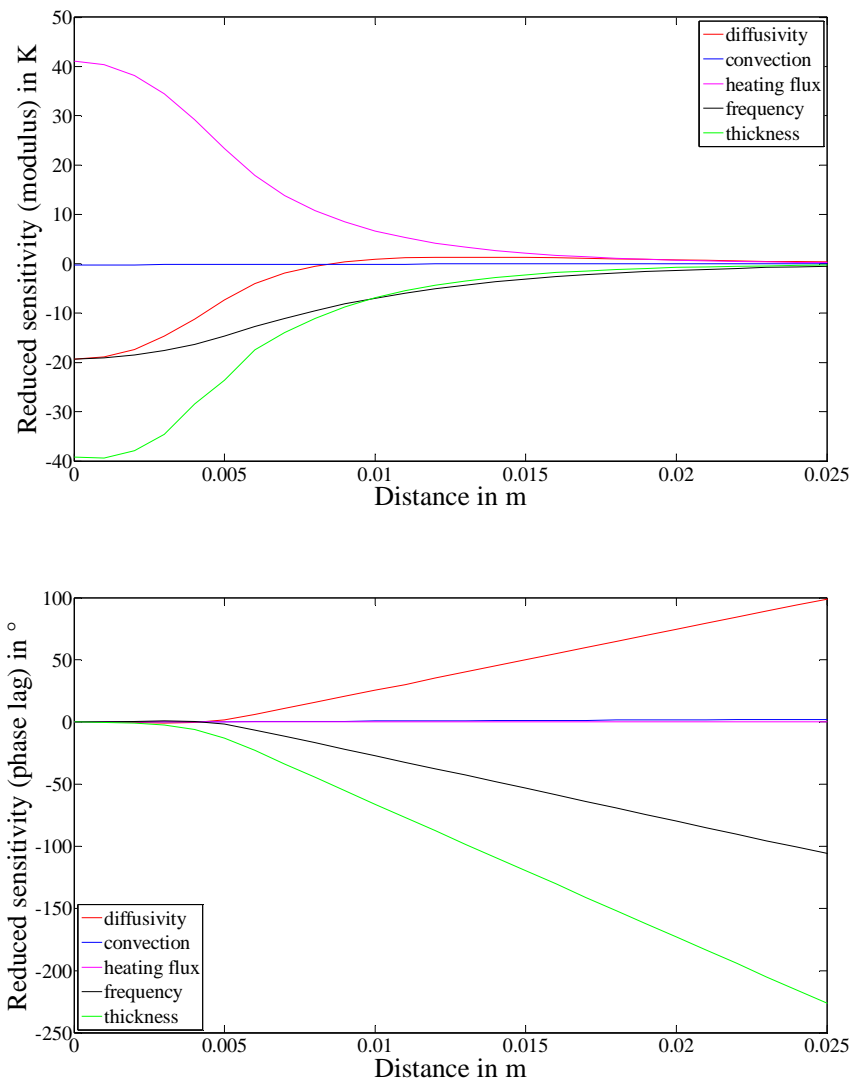
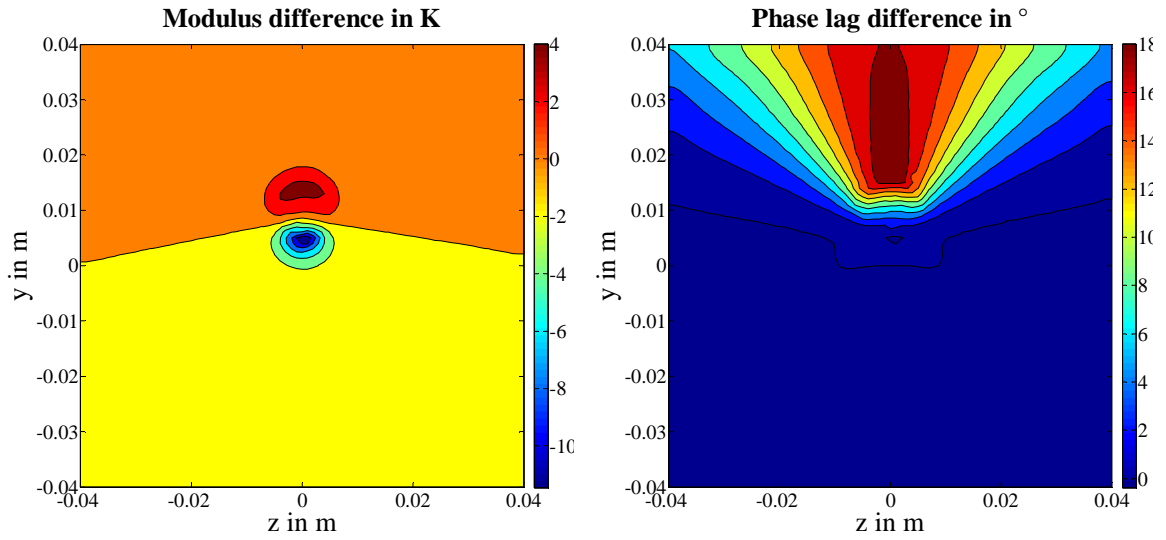
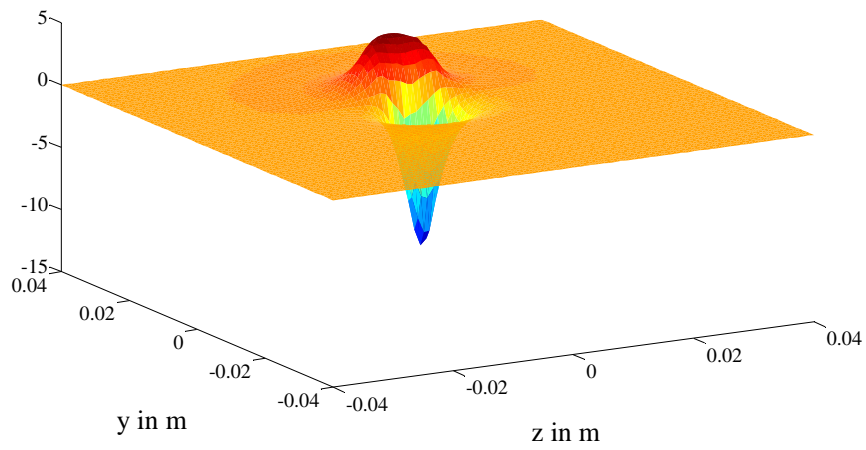


Figure 3 Reduced sensitivity



Modulus difference in K



Phase lag difference in °

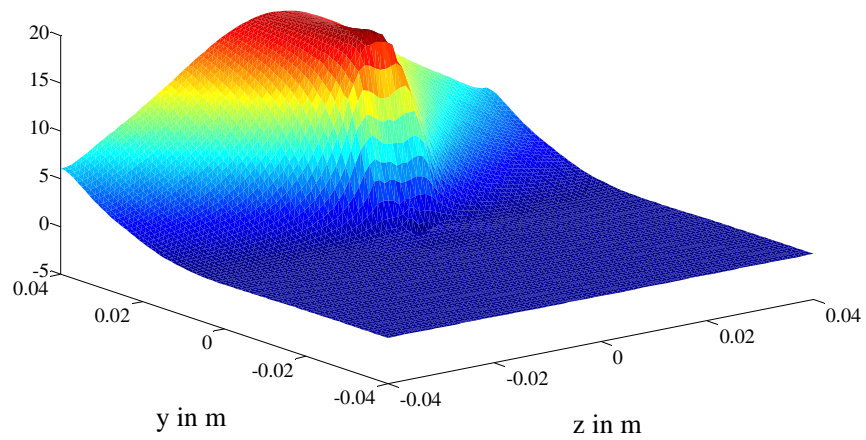
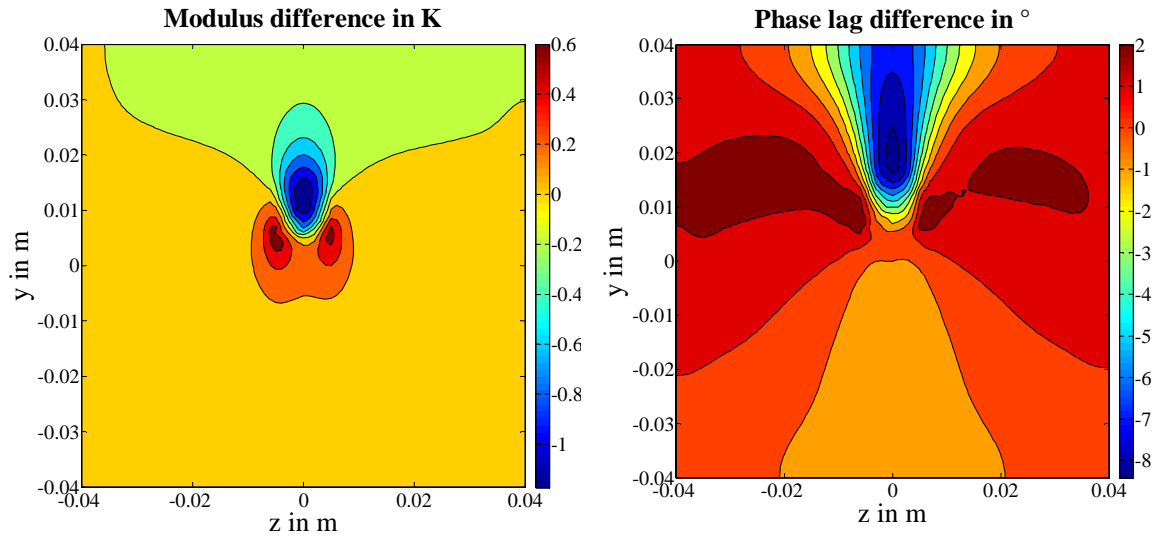
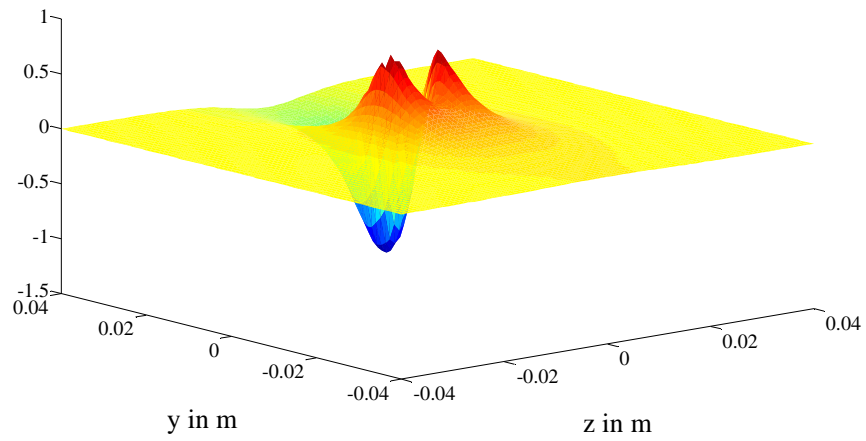


Figure 4 Inclusion detection



Modulus difference in K



Phase lag difference in $^{\circ}$

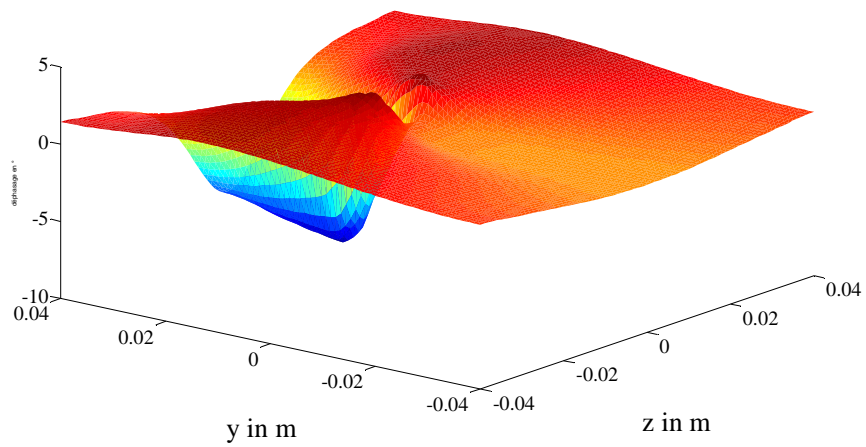


Figure 5 Detection of fibres misalignment in an orthotropic composite material

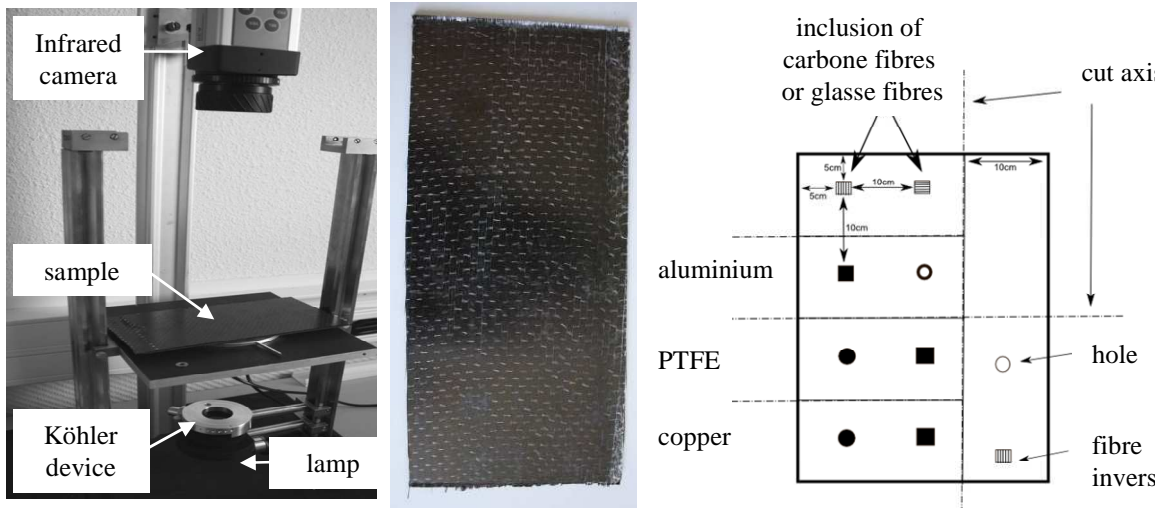


Figure 6 Experimental device and studied sample

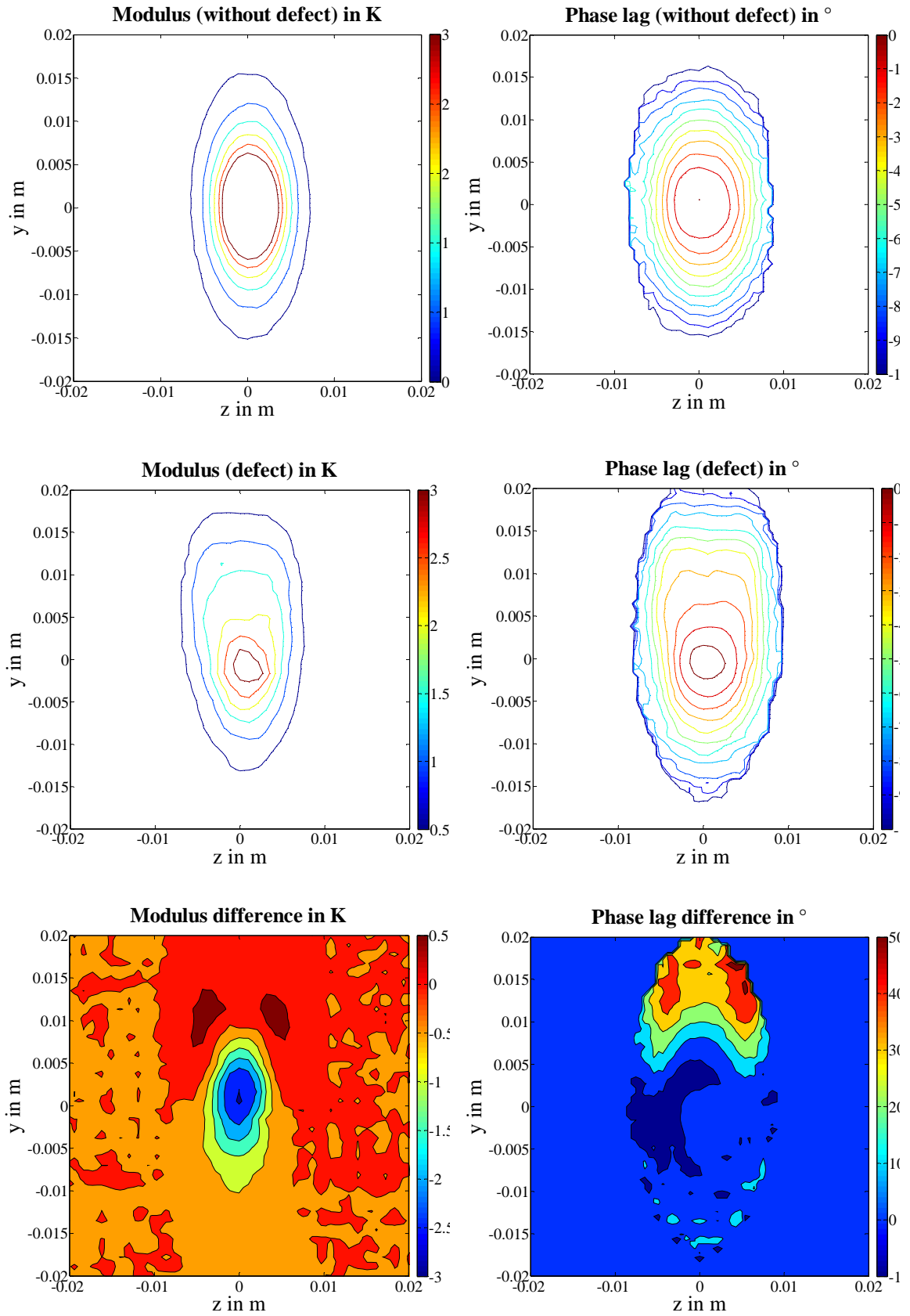


Figure 7 Differences for both modulus and phase lag experimental cartographies